International Journal of Refractory Metals & Hard Materials 72 (2018) 9–14

Contents lists available at ScienceDirect

International Journal of Refractory Metals & Hard Materials

journal homepage: www.elsevier.com/locate/IJRMHM

Synthesis and characterization of porous tungsten carbide with added tungsten silicides

Jelena Luković[a,*], Dubravka Milovanović[a], Ravi Kumar[b], Mirjana Kijevčanin[c], Ivona Radović[c], Branko Matović[a], Tatjana Volkov-Husović[b]

[a] Vinča Institute of Nuclear Sciences, Belgrade, Serbia
[b] Indian Institute of Technology-Madras (IIT Madras), Chennai, India
[c] Faculty of Technology and Metallurgy, University of Belgrade, Serbia

A B S T R A C T

Porous materials made of commercial tungsten carbide (WC) with the addition of thermally obtained tungsten silicides (WSi_2 and W_5Si_3) were made. The main research's contribution is firstly finding optimal conditions for synthesis tungsten silicides from elementary powders, and lately obtaining porous materials with excellent cavitation resistance. A phase transformation during synthesis of silicides was studied by changing temperature and time of heating. Obtained silicides were added to WC in different mass percentages. Mixtures were spark plasma sintered. Nanoindentation tests were performed on sintered samples, as well as cavitation erosion testing accompanied by measuring of mass changes and the profilometry measurements to scan the surface. Microstructure and morphology were determined by scanning electron microscopy (SEM), while porosity percentages based on SEM images were calculated by computer software QWin.

1. Introduction

In metallurgical industry and in advanced technologies, used materials are frequently subjected to extreme conditions such as chemical, mechanical exposures, and operation under high temperatures [1]. Therefore, required materials have to be carefully chosen. Some refractory materials which possess high melting points (> 1800 °C), chemically inertness, high hardness as well as toughness and good wear resistant satisfy the requirements for extreme usage conditions [2]. Tungsten carbide phases, WC with the melting point above 2785 °C, tungsten disilicide (WSi_2) with the melting point above 2160 °C and petatungsten trisilicide (W_5Si_3) with the melting point above 2320 °C seems appropriate to operate in these conditions. WC has very high hardness, low friction coefficient, low reactivity, high oxidation resistance, and good thermal and electrical conductivity [2]. WSi_2 has low electrical resistivity and good thermal stability. Tungsten dislicide is examined as a protective coating on W-based alloys because of its excellent oxidation resistance [3,4,5,6].

During oxidation, two separate phases can be distinguished. At lower temperatures, a protective layer of SiO_2 is formed, and at higher temperatures evaporative oxides SiO, WO_2, and WO_3 are formed [4,5,6]. Kim et al. discussed WSi_2 transformation into W_5Si_3 at elevated temperatures, what Kharatyan et al. experimentally confirmed [4,7]. W_5Si_3 coatings have great abrasive and adhesive wear resistance [8].

Densification of tungsten carbide has been investigated systematically [9,10,11,12] often as cemented carbide, with an addition of Co or similar low-melting point binders [13,14,15] but corrosion and oxidation occur preferentially in the binder phase [16]. For this reason, WSi_2 and W_5Si_3 intrude as suitable materials for mixing with WC in order to overcome the problem of oxidation in extreme conditions for application in the metal and cutting tools industries.

On the other hand, it was found that tungsten carbide has potential catalytic behavior similar to the one typical for metals of the platinum group [17] the great number of research came after in order to replace noble metals as catalysts [18,19,20,21,22]. Levy and Boudart [17] also found that catalytic activity of WC is much lower than that of platinum metal. Later, it was discovered that the surface area of tungsten carbide is one of the key factors that determine its catalytic activity [23,24] and that electrocatalytic properties of porous tungsten carbide are higher than that of solid granular WC particle [25,26,27].

In this paper, authors present a synthesis of W-silicides powder as a sintering additive and later spark plasma sintering of commercial tungsten carbide with synthesized tungsten silicide powders. The synthesis of tungsten silicides consists of simple thermal treatment of a mixture of tungsten and silicon powders. The effect of the temperature and duration of heat treatment on a composition of the obtained

* Corresponding author.
E-mail address: jelenal@vinca.rs (J. Luković).

https://doi.org/10.1016/j.ijrmhm.2017.12.001
Received 3 May 2017; Received in revised form 13 November 2017; Accepted 3 December 2017
Available online 06 December 2017

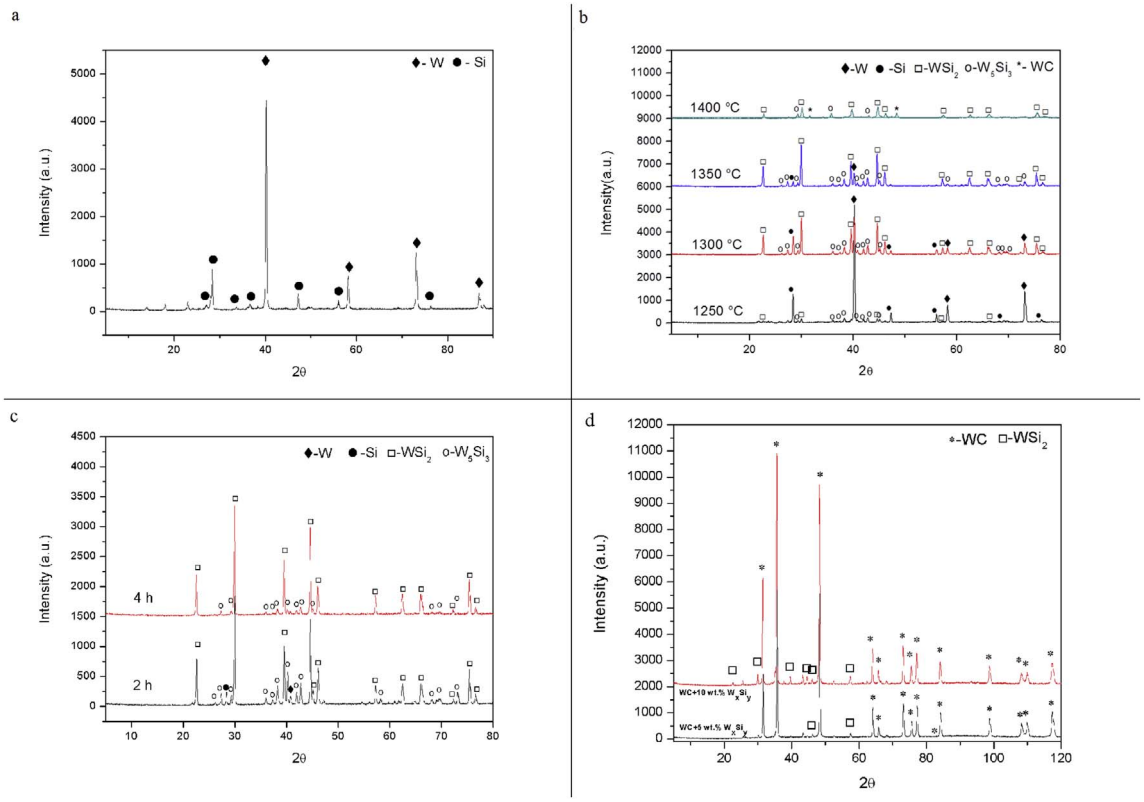

Fig. 1. a) XRD pattern of starting powders after homogenization procedure b) XRD patterns of samples obtained after heating at different temperatures for 2 h in an argon atmosphere. c) XRD patterns of samples obtained at 1350 °C for different amounts of heating time.

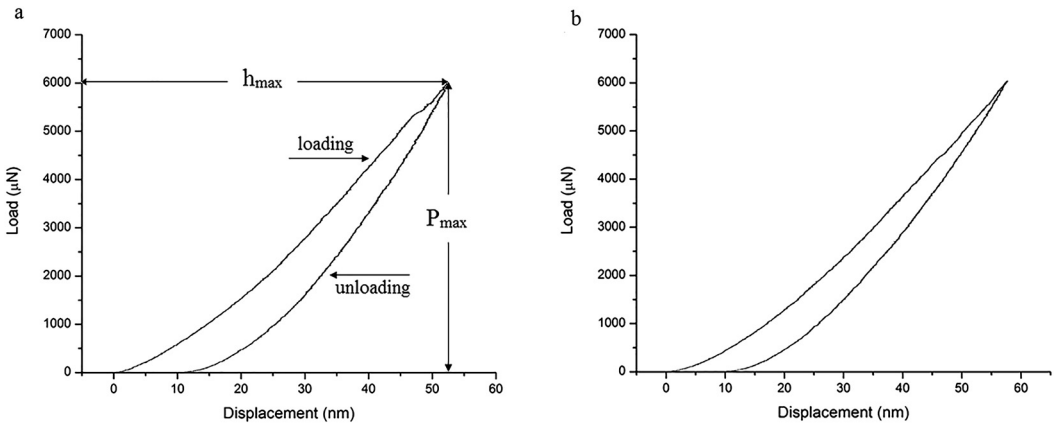

Fig. 2. Load–displacement curves of sintered samples: a) WC + 5 wt% W_xSi_y. b) WC + 10 wt% W_xSi_y.

powders were studied. The powder obtained under chosen optimal conditions was used as a sintering additive. According to our knowledge, this composite is made and sintered for the first time. Hardness and Young's elastic modulus were determined. Cavitation erosion test was performed to investigate behavior and possible application of this composite material under extreme conditions of the cavitation exposure. Surface topography scanned and characterized before and after each cavitation test to follow any changes in the materials' surface.

2. Materials and methods

2.1. Preparation of tungsten silicide powder

For this study, commercial tungsten powder (Koch-Light Laboratories, LTD, purity 99.9%) of average grain size of 1 μm according to manufacturer specification, and commercial silicon powder were used as starting materials for the synthesis of tungsten silicide powders. They were homogenized in acetone for 24 h. Starting powders were used in the stoichiometric ratio while the ball-to-powder ratio was 5:1. After homogenization and air drying, acetone evaporated. The prepared mixture was thermally treated at different temperatures ranging from 1250 to 1400 °C, with the increment of 50 °C. The heating rate was 10 °C/min. The mixture was placed in a tube furnace. The heat treatment was conducted in argon flow for different holding times — 2 and 4 h. After the treatment, the furnace was cooled to the room temperature.

2.2. Preparation of the SPS composites

Obtained tungsten silicide powders were mixed and homogenized with commercial tungsten carbide powder. The amount of added tungsten silicides were 5 and 10 wt%. These mixtures were spark

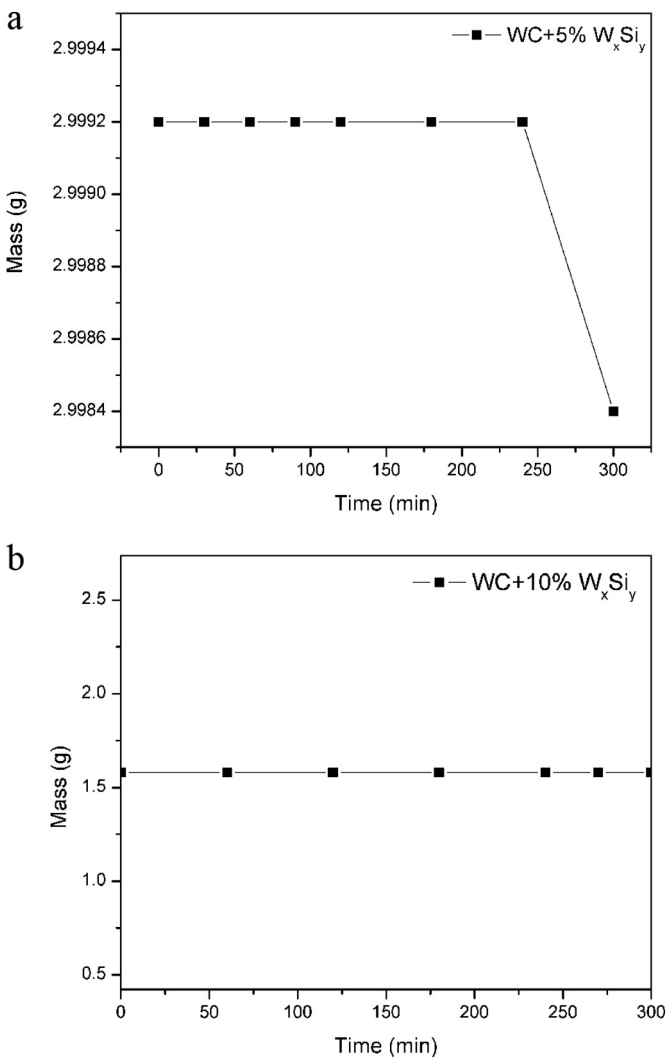

Fig. 3. Mass loss of sintered samples during the cavitation erosion testing: a) WC + 5 wt % W_xSi_y b) WC + 10 wt% W_xSi_y.

plasma sintered (SPS). SPS was carried out using Dr. Sinter SPS-625 (Fuji Electronic Co. Ltd., Japan) at 1600 °C at a heating rate of 100 °C/min and a load of 50 MPa for 5 min in a vacuum.

2.3. XRD analysis

All powders and solids were characterized by X-ray diffraction (XRD) using X-ray diffractometer (Rigaku Ultima IV, Japan) with Cu $K\alpha_1$ radiation and Ni filter. The scanning of samples was done at a speed 2°/min in a range of diffraction angle 2θ 5–80°, with the angular resolution of 0.02° for all XRD tests.

2.4. Nanoindentation measurements

After sintering, obtained compacts were investigated using a Berkovich indenter. Maximum load used was 6000 μN. Load pattern was triangular with 10 s of loading, 10 s of unloading and with no holding time. There were 15 indents per sample. There was 10 μm of a gap between the indents. Elastic modulus and hardness of materials were determined by the well-known Oliver-Pharr method [28,29] from an average value of those 15 indents.

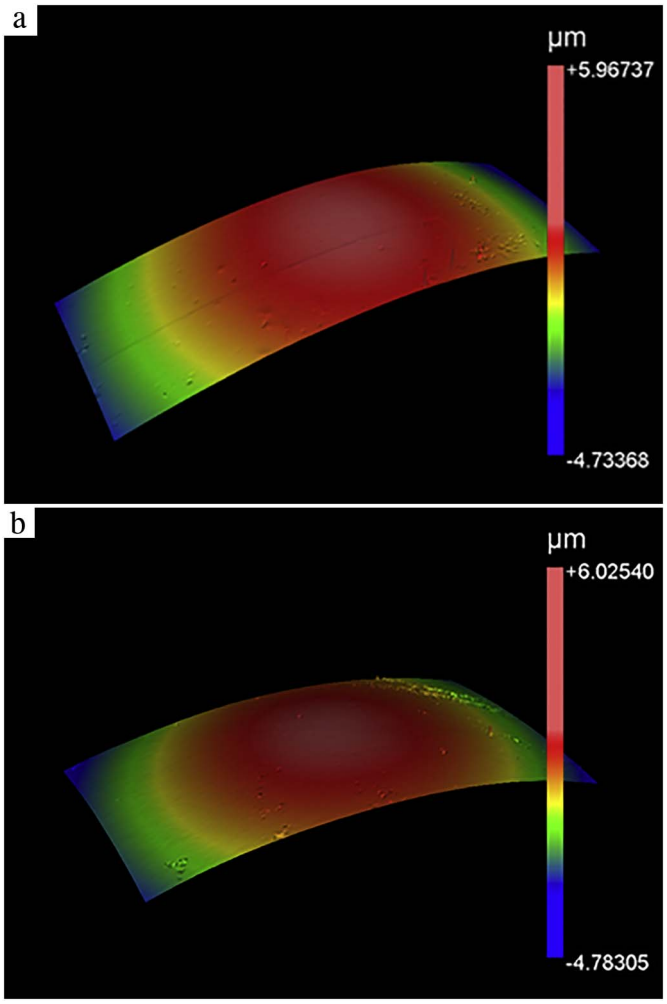

Fig. 4. 3D projection of 5% WSi surface topography after final cavitation.

2.5. Cavitation erosion testing and profilometry

The fluid dynamic system of the cavitation erosion methodology used here to produce ultrasonic cavitations is explained in detail elsewhere [30]. The cavitation erosion testing was accomplished utilizing the recommended standard values: the frequency of the vibration was 20 ± 0.2 kHz, the amplitude of the vibration at the top of the transformer was 50 ± 2 μm, the gap between the test specimen and the transformer was 5.0 mm, the temperature of water in the bath was 25 ± 1 °C. These parameters were controlled throughout the testing process. The measurements were performed after subjecting each test specimen to cavitation for 30 min. The cumulative duration of the tests was 300 min.

Mass losses of the test specimens were done on an analytical balance with an accuracy of ± 0.1 mg. The measurements were performed after subjecting each test specimen to cavitation for 30 min.

Profilometry was used to scan the surface topography, obtain an image and three-dimensional profile of the tested surface before and after each cavitation. Surface topography of WC/WSi_x was analyzed using a non-contact 3D optical surface profiler (Zygo New View 7100, USA). Surface parameters (average surface roughness, R_a and corresponding root-mean-square roughness, rms) were determined using MetroPro software (licensed by Zygo Corporation, USA).

2.6. Microstructure and phase composition

The microstructure and chemical composition of the obtained

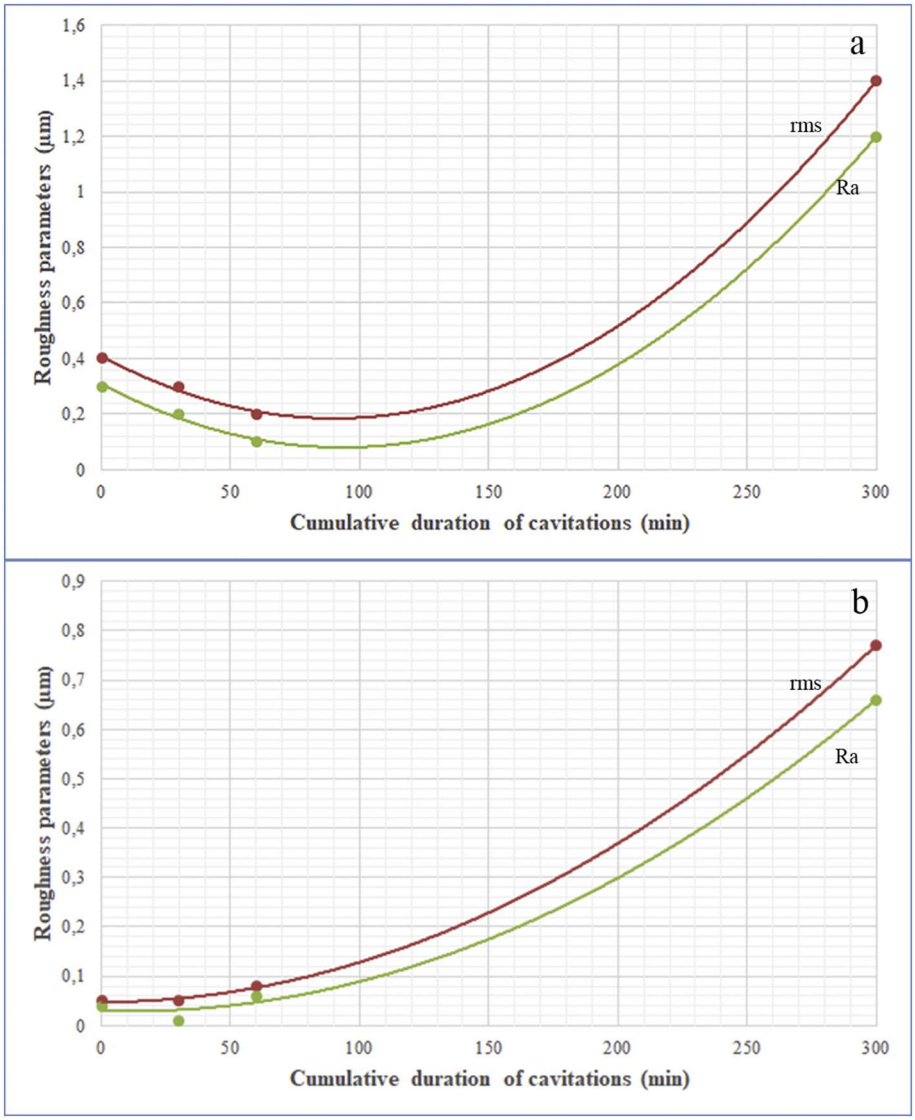

Fig. 5. Change in surface roughness parameters during cavitation erosion testing for sintered samples: a) WC + 5 wt% W_xSi_y b) WC + 10 wt% W_xSi_y.

sintered solids were examined using a Tescan Vega TS 5130MM scanning electron microscope coupled by EDS Oxford Instruments INCA PentaFET-x3. The porosity percentage of samples was calculated by the quantitative image analysis processing using Q-win computer-assisted image analyzer. The porosity was determined from SEM micrographs.

3. Results and discussion

3.1. XRD analysis of tungsten silicides

XRD analysis was performed to follow every step of the synthesis of materials, including the effect of temperature and annealing time on phase evolution of tungsten silicides. According to results of XRD analysis, it is possible to select the optimal conditions for preparing tungsten based silicides.

Fig. 1a shows the composition of dried powder after mixing of elementary tungsten and silicon. It reveals that starting powders did not react with acetone during the mixing process.

Fig. 1b shows the XRD patterns of samples after heating at different temperatures for 2 h in an argon flow and presents the effect of temperature on phase composition. Tungsten and silicon (1250 °C) react to form tungsten dislicide (WSi_2) and pentatungsten trisilicide (W_5Si_3) at higher temperatures (1300 to 1400 °C). The temperature of 1400 °C is sufficiently high for conversion of starting materials to tungsten based silicides without any remains of unreacted tungsten and silicon, but the impurities like WC are present in a material, probably due to present carbon content in the furnace, so reaction with tungsten occurred to form WC.

Considering the presence of impurities at 1400 °C, and only small amount of elementary W and Si in sample heated for 2 h at 1350 °C, the influence of holding time on phase evolution, while the temperature was constant has been tested. It was concluded that 4 h of heating time at this temperature leads to complete conversion of those elementary powders to WSi_2 and W_5Si_3, which is clearly confirmed at Fig. 1c.

After choosing powder, obtained at 1350 °C and 4 h of heating time, as optimal, and mixing with commercial tungsten carbide powder in different mass percentages, and later after sintering, as stated before, composition of solid sample was determined by X-ray diffraction, as shown at Fig. 1d.

3.2. Nanoindentation results

For simplicity of displaying the results, typical examples of load–-displacement curves obtained from nanoindentation of sintered samples with 5 and 10 wt% of silicides are presented in Fig. 2.

As loading takes place, deformation occurs both elastically and plastically, so final displacement is less than maximum one [31].

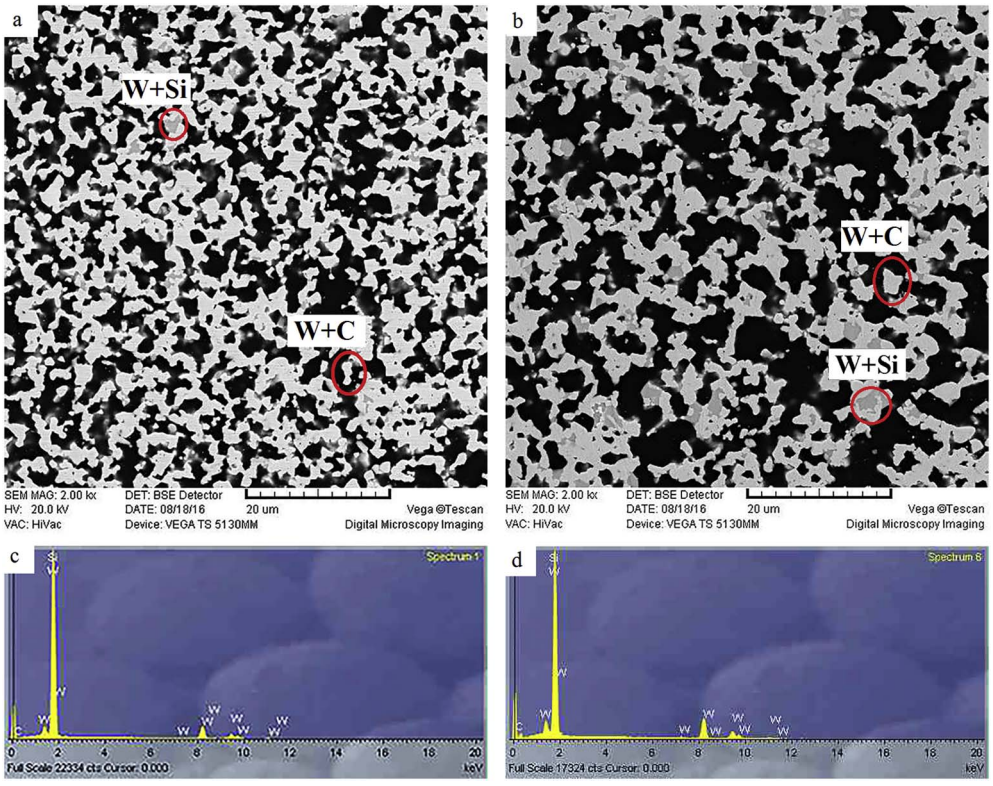

Fig. 6. SEM micrographs of sintered samples: a) WC + 5 wt% W_xSi_y b) WC + 10 wt% W_xSi_y. EDS analysis of sintered samples: c) WC + 5 wt% W_xSi_y d) WC + 10 wt% W_xSi_y.

Table 1
The porosities of sintered samples.

Sample	Porosity, A_A (%)
WC + 5 wt% W_xSi_y	43.5 ± 12.9
WC + 10 wt% W_xSi_y	36.7 ± 3.7

Oliver–Pharr method [28] was used to calculate the hardness and the elastic modulus from the load-displacement curves for each indentation.

The slope of the unloading curve at maximum load (dP/dh) gives Stiffness (S).

$$S = \frac{dP}{dh}$$

This value is used in to calculate reduced Young's elastic modulus (E_r) using [29]:

$$E_r = \frac{1}{\beta}\frac{\sqrt{\pi}}{2}\frac{S}{\sqrt{A_p(h_c)}}$$

Where $A_p(h_c)$ is the projected area of the indentation at the contact depth h_c, and β is a geometrical constant on the order of unity. And finally, actual elastic modulus (E) is calculated:

$$\frac{1}{E_r} = \frac{(1-\nu^2)}{E} + \frac{(1-\nu_i^2)}{E_i}$$

Elastic moduli (Ei) and Poisson's ratio (ν_i^2) of an indenter are taken as 1141 GPa and 0.07 respectively. Poisson's ratio used for the sample (ν) is 0.24.

The calculated average elastic modulus (and related standard deviation values) for the samples with 5 and 10 wt% of tungsten silicides are, respectively, 393.27 ± 5.31 and 340.79 ± 6.67 GPa.

The average hardness, where hardness is presented as a function of a projected area of the hardness impression, is estimated from:

$$H = \frac{P_{max}}{A_r}$$

Where P_{max} is maximum load, and A_r represents the indentation area.

Calculated average values of hardness for samples with 5 and 10 wt % of silicides, with corresponding standard deviations, are 16.71 ± 1.42 and 16.48 ± 1.67 GPa, respectively.

In literature there are lots of studies dedicated to finding correlation of the orientation of WC crystals and their hardness, namely to understand the relation between microstructure and hardness of a material [32,33,34]. These studies are based on an investigation of WC in form of cemented carbide, preferably WC-Co. They found that basal plane hardness is higher than one for a prismatic plane. In our study, hardness measurements are surface measurements, and values were determined by the average of 15 readings for each test condition. So, the hardness approaches an average value for both basal and prismatic planes, including hardness of a binder phase.

3.3. Cavitation erosion test

The mass loss during the cavitation erosion experiment is illustrated in Fig. 3. The data shows that the sample exhibited excellent resistance to the erosion cavitation testing. The mass loss was minimal about 0.0008 g (0.027% mass loss of the starting material) after 300 min of testing for the sample with 5 wt% of added silicides. Sample with 10 wt % of added silicides recorded no weight loss during the same experimental test.

3.4. Surface topography analysis – non-contact profilometry

Effects of cavitation process on materials' surface features and characteristic parameters were determined by optical white-light profilometry, prior and after each cavitation step.

Example of the three-dimensional projection is presented in Fig. 4.

Correlation between mass loss and surface parameters due to cavitation can be observed. Hence, when there is an overall change in

surface roughness for factor 3.5, there is the corresponding decrease in mass of sample with 5 wt% of added silicides, Fig. 5a) Also, changes of surface parameters for factor 1.2 is corresponding to no significant mass loss of sample material with 10 wt% of added silicides, Fig. 5b) Surface profile parameters Ra, and rms are shown in the Fig. 5a) and b) for samples with 5 and 10 wt% of added silicides.

3.5. Microstructure and phase composition

The SEM micrographs of sintered samples are shown in Fig. 6. For each sample same magnifications are shown. Obtained samples have different porosities but with similar microstructure.

EDS analysis, presented in Fig. 6b and c. showed that light gray regions consist of W and C, while dark gray regions are made of W and Si.

Porosity percentage of the projected area of examined sample was calculated by the quantitative image analysis processing using the standard image analysis technique with adequate computer software (QWin). The porosity of samples was determined from SEM micrographs (Fig. 6a and b) which were taken at a magnification of 2000 ×. Calculated results are given in Table 1. These results should be taken as estimated values.

4. Conclusion

In this work homemade mixtures of WSi_2 and W_5Si_3 were made. Change in temperature and heating time was observed to find optimal experimental conditions for synthesis of those silicides. After adding them to commercial WC powder, and spark plasma sintering, porous materials were made. Calculated porosities of materials were 43.5% for the sample with 5 wt% and 36.7% for the sample with 10 wt% of additives. These materials exhibit great cavitation erosion resistance presented by the minimal loss of mass. The results show that in spite of high porosity obtained materials have an excellent resistance to the erosion cavitation testing. According to authors' knowledge, this is first time mixture of tungsten carbide and tungsten silicides is made, so these materials have a potential for further researches in improving or changing some of the material properties.

Acknowledgement

This project was financially supported by the Ministry of Education and Science of the Republic of Serbia (Project Number: 45012).

References

[1] S. Oyama, Introduction to the chemistry of transition metal carbides and nitrides, The Chemistry of Transition Metal Carbides and Nitrides, Springer, Netherlands, 1996, pp. 1–27.
[2] H.O. Pierson, Handbook of Refractory Carbides and Nitrides: Properties, Characteristics, Processing and Applications, Elsevier Inc., 1996.
[3] C. Gelain, A. Cassuto, P. Le Goff, Kinetics and mechanism of the low-pressure, high-temperature oxidation of tungsten silicides-III, Oxid. Met. 3 (2) (1971) 153–169.
[4] S.L. Kharatyan, H. Chatilyan, A.B. Harutyunyan, High-temperature silicon diffusivities in Mo_5Si_3 and W_5Si_3 phases, Diffus. Defect Data, Part A 194–199 (2001) 1557–1562.
[5] K.H. Lee, J.K. Yoon, J.K. Lee, J.M. Doh, K.T. Hong, W.Y. Yoon, Growth kinetics of W_5Si_3 layer in WSi_2/W system, Surf. Coat. Technol. 187 (2–3) (2004) 146–153.
[6] J.K. Yoon, K.W. Lee, S.J. Chung, I.J. Shon, J.M. Doh, G.H. Kim, Growth kinetics and oxidation behavior of WSi_2 coating formed by chemical vapor deposition of Si on W substrate, J. Alloys Compd. 420 (1–2) (2006) 199–206.
[7] H.S. Kim, J.K. Yoon, G.H. Kim, J.M. Doh, S.I. Kwun, K.T. Hong, Growth behavior and microstructure of oxide scales grown on WSi_2 coating, Intermetallics 16 (3) (2008) 360–372.
[8] L. Cai, Wang, Microstructure and dry-sliding wear resistance of laser clad tungsten reinforced W_5Si_3/W_2Ni_3Si intermetallic coatings, Appl. Surf. Sci. 235 (4) (2004) 501–506.
[9] J. Poetschke, V. Richter, T. Gestrich, A. Michaelis, Grain growth during sintering of tungsten carbide ceramics, Int. J. Refract. Met. Hard Mater. 43 (2014) 309–316.
[10] Y. Jiang, J.F. Yang, Z. Zhuang, R. Liu, Y. Zhou, X.P. Wang, Q.F. Fang, Characterization and properties of tungsten carbide coatings fabricated by SPS technique, J. Nucl. Mater. 433 (1–3) (2013) 449–454.
[11] A. Gubernat, P. Rutkowski, G. Grabowski, D. Zientara, Hot pressing of tungsten carbide with and without sintering additives, Int. J. Refract. Met. Hard Mater. 43 (2014) 193–199.
[12] L. Girardinia, M. Zadraa, F. Casaria, A. Molinarib, SPS, binderless WC powders, and the problem of sub carbide, Met. Powder Rep. 63 (4) (2008) 18–22.
[13] J.Y. Suh, S.E. Shin, D.H. Bae, Fabrication of tungsten-based composites by solid binder mixing and sintering, Powder Technol. 289 (2015) 401–405.
[14] S. Bukolaa, B. Merzouguic, A. Akinpelua, M. Zeamaa, Cobalt and nitrogen Co-doped tungsten carbide catalyst for oxygen reduction and hydrogen evolution reactions, Electrochim. Acta 1 (2016) 1113–1123.
[15] X. Yuana, C. Weib, D. Zhanga, J. Zhuc, X. Gaoc, Characterization and comparison of grain boundary character distributions in cemented carbides with different binder phases, Comput. Mater. Sci. 93 (2014) 144–150.
[16] H. Suzuki, Cemented Carbide and Sintered Hard Materials, Maruzen Publishing Compan, Tokyo, 1986.
[17] R.B. Levy, M. Boudart, Platinum-like behavior of tungsten carbide in surface catalysis, Science 181 (4099) (1973) 547–549.
[18] Y. Wang, C. He, A. Brouzgou, A. Liang, R. Fu, D. Wu, P. Tsiakaras, S. Song, A facile soft-template synthesis of ordered mesoporous carbon/tungsten carbide composites with high surface area for methanol electrooxidation, J. Power Sources 200 (2012) 8.
[19] E. Weigert, A. Stottlemyer, M. Zellner, J. Chen, Tungsten monocarbide as potential replacement of platinum for methanol electrooxidation, J. Phys. Chem. C 111 (2007) 14617.
[20] Z. Chen, M. Qin, P. Chen, B. Jia, Q. He, X. Qu, Tungsten carbide/carbon composite synthesized by combustion-carbothermal reduction method as electrocatalyst for hydrogen evolution reaction, Int. J. Hydrog. Energy 41 (30) (2016) 13005–13013.
[21] C. Tang, D. Wang, Y. Wu, B. Duan, Tungsten carbide hollow microspheres as electrocatalyst and platinum support for hydrogen evolution reaction, Int. J. Hydrog. Energy 40 (2015) 3229–3237.
[22] F. Harnisch, G. Sievers, U. Schröder, Tungsten carbide as electrocatalyst for the hydrogen evolution reaction in pH neutral electrolyte solutions, Appl. Catal. B Environ. 89 (2009) 455–458.
[23] I. Nikolov, T. Vitanov, V. Nikolova, The effect of the method of preparation on the catalytic activity of tungsten carbide for hydrogen evolution, J. Power Sources 5 (1980) 197–206.
[24] I. Nikolov, V.T. Nikolova, The effect of method of preparation on the catalytic activity of tungsten carbide, J. Power Sources 4 (1979) 65–75.
[25] C. Ma, W.M. Zhang, G. Li, Y. Zheng, B. Zhou, D. Cheng, Preparation of hollow global tungsten carbide (WC) catalysts with meso-porosity and its characterization, Acta Chim. Sin. 63 (13) (2005) 1151–1154.
[26] J.P. Bosco, K.S.M.U.W. Sasaki, J.G. Chen, Synthesis and characterization of three-dimensionally ordered macroporous (3DOM) tungsten carbide: application to direct methanol fuel cells, Chem. Mater. 22 (3) (2010) 966–973.
[27] D.J. Ham, R. Ganesan, J.S. Lee, Tungsten carbide microsphere as an electrode for cathodic hydrogen evolution from water, Int. J. Hydrog. Energy 33 (23) (2008) 6865–6872.
[28] W.C. Oliver, G.M. Pharr, An improved technique for determining hardness and elastic modulus using load and displacement sensing indentation experiments, J. Mater. Res. 7 (06) (1992) 1564–1583.
[29] W.C. Oliver, G.M. Pharr, Measurement of hardness and elastic modulus by instrumented indentation advances in understanding and refinements to methodology, J. Mater. Res. 19 (07) (2004) 3–20.
[30] S. Martinovic, M. Vlahovic, M. Dojcinovic, T. Volkov-Husovic, Thermomechanical properties and cavitation resistance of a high-alumina low-cement castable, Int. J. Appl. Ceram. Technol. 8 (5) (2010) 1115–1124.
[31] M.G. Gee, B. Roebuck, P. Lindahl, H.-O. Andren, Constituent phase nanoindentation of WC/Co and Ti(C,N) hard metals, Mater. Sci. Eng. A 209 (1996) 128–136.
[32] V. Bonache, E. Rayón, M.D. Salvador, D. Busquets, Nanoindentation study of WC–12Co hardmetals obtained from nanocrystalline powders: evaluation of hardness and modulus on individual phases, Mater. Sci. Eng. A 527 (12) (2010) 2935–2941.
[33] A. Duszováa, R. Halgaša, M. Bľandaa, P. Hvizdoša, F. Lofaja, J. Dusza, Nanoindentation of WC–Co hardmetals, J. Eur. Ceram. Soc. 33 (12) (2013) 2227–2232.
[34] J. Roaa, E. Jimenez-Piquea, C. Vergea, J.M. Tarragóa, A. Mateoa, J. Fairc, L. Llanesa, Intrinsic hardness of constitutive phases in WC–Co composites: nanoindentation testing,statistic alanalysis, WC crystal orientation effects and flow stress for the constrained metallic binder, J. Eur. Ceram. Soc. 35 (2015) 3419–3425.